Iron(II) Oxidation by H Chain Ferritin: Evidence from Site-Directed Mutagenesis That a Transient Blue Species Is Formed at the Dinuclear Iron Center†

A. Treffry,* Z. Zhao, M. A. Quail, J. R. Guest, and P. M. Harrison

The Krebs Institute, Department of Molecular Biology and Biotechnology, University of Sheffield, Sheffield S10 2TN, U.K.

Received June 5, 1995; Revised Manuscript Received September 6, 1995®

ABSTRACT: The iron storage molecule, ferritin, consists of an iron core surrounded by a shell of 24 protein subunits, which, in mammals, are of two types, H and L. Prior to storage of iron as a hydrous ferric oxide within the protein shell, Fe(II) is catalytically oxidized at dinuclear centers within H chains. When 48 Fe(II) atoms/molecule were added to 1 μM recombinant human H chain apoferritin (apo-HuHF), in 0.1 M Mes (pH 6.5), oxidation was 80% complete within about 0.2 s while 99% of the Fe(II) was oxidized within 10 s. A broad visible absorption band (400−800 nm, with a maximum at 650 nm) appeared during the fast phase of Fe(II) oxidation. It reached a plateau at 0.2−0.3 s and then declined while Fe(II) oxidation proceeded to completion and absorbance in the near-UV (300−400 nm) increased. The transient visible species was not observed when Tyr-34 was replaced by phenylalanine or when other conserved amino acids at the ferroxidase centers were substituted by residues which are unable to bind iron or which alter the charge balance. When a second increment of 48 iron atoms was added, 10 min after the first, the visible absorbance was absent and the rate of oxidation slower. Restoration of full oxidative activity took over 24 h. The data indicate that the fast oxidation of Fe(II) by apo-HuHF and the transient visible absorbance associated with it are due to Fe(II) oxidation at the ferroxidase centers.

The iron storage protein, ferritin, is found throughout the living kingdom. The iron-free protein, apoferritin, is a symmetrical, hollow sphere composed of 24 polypeptide chains. Each subunit has five α-helices (A−E), of which helices A−D are arranged as a four-helix bundle. The central 8 nm diameter cavity is capable of storing up to 4500 Fe(III) atoms as an inorganic mineral core of hydrous ferric oxide (ferrihydrite). *In vitro*, iron is taken up as Fe(II) and catalytically oxidized within the protein shell prior to deposition as a stable mineral. Studies with site-directed variants have indicated that oxidation occurs at di-iron sites (the ferroxidase centers), which are situated centrally within the four-helix bundles of H-type chains (Lawson et al., 1991; Bauminger et al., 1991, 1993, 1994; Hempstead et al., 1994). Mammalian and amphibian ferritins are heteropolymers containing L-type chains (lacking catalytic centers) as well as the H-type chains, whereas all known bacterial and plant ferritins are homopolymers of only H-type chains (Andrews et al., 1992).

Iron incorporation into ferritin has been analyzed usually by measuring the increase in absorbance due to the presence of oxidized species: Fe(III) dimers, small oligomers, and the larger polymeric clusters or "iron cores". Such measurements have been made at a single wavelength in the range 310−360 nm [e.g. Treffry et al. (1989) and Levi et al. (1988)], at 420 nm (Macara et al., 1972; Waldo & Theil, 1993), and at 550 nm (Waldo & Theil, 1993; Bauminger et al., 1993). Relative rates of iron oxidation have also been estimated by measuring residual Fe(II), as colored complexes with Fe(II) chelators (Niederer, 1970; Bauminger et al., 1993), and by monitoring oxygen consumption (Sun et al., 1993; Waldo & Theil, 1993).

Intermediates of iron oxidation and core formation identified by UV-difference, Mössbauer, EPR,[1] EXAFS, and Raman spectroscopy include isolated Fe(III) atoms (Rosenberg & Chasteen, 1982; Jacobs et al., 1989; Sun & Chasteen, 1994), Fe(III)/Fe(II) (Hanna et al., 1991; Sun & Chasteen, 1994) and Fe(III)/Fe(III) dimers (Bauminger et al., 1989, 1993, 1994; Treffry et al., 1992), an Fe(III)−tyrosinate complex (Waldo et al., 1993), and Fe(III) clusters (Bauminger et al., 1989, 1994; Yang et al., 1987). However, data for the first 30 s after Fe(II) addition were scarce until the recent appearance of three reports of stopped-flow spectroscopic studies of iron oxidation by EcBFR (Le Brun et al., 1993), HuHF (Bauminger et al., 1993), and BfHF (Waldo & Theil, 1993). These showed that, when 48 Fe(II) atoms/molecule were added (enough to saturate the ferroxidase centers and undergo a single cycle of Fe(II) oxidation), iron oxidation was completed within 20 s. In HuHF, a transient, visible absorbance, reaching a maximum at 0.2−0.3 s and then decaying, was observed after mixing apo-HuHF and 24 Fe(II) atoms/molecule (Bauminger et al., 1993). In BfHF, the formation of a transient species absorbing at 550 nm was studied (Waldo & Theil, 1993) following its assignment, by Raman spectroscopy, as a tyrosine → Fe(III) charge transfer complex (Waldo et al., 1993).

Further investigations of factors affecting the formation of the transient species in HuHF are described here, including

† This work was supported by grants from The Wellcome Trust (035978 to A.T. and 040204 to J.R.G., A.T., and P.M.H.).

® Abstract published in *Advance ACS Abstracts,* November 1, 1995.

[1] Abbreviations: HuHF, recombinant human H chain ferritin homopolymer; HoLF, recombinant horse L chain ferritin homopolymer; HoSF, horse spleen ferritin; EcFTN, *Escherichia coli* non-heme ferritin; EcBFR, *E. coli* bacterioferritin (heme-containing); BfHF, recombinant bullfrog H chain ferritin homopolymer; apo-HuHF, iron-free HuHF; EPR, electron paramagnetic resonance; EXAFS, extended X-ray absorption fine structure; ACP, acyl carrier protein.

0006-2960/95/0434-15204$09.00/0

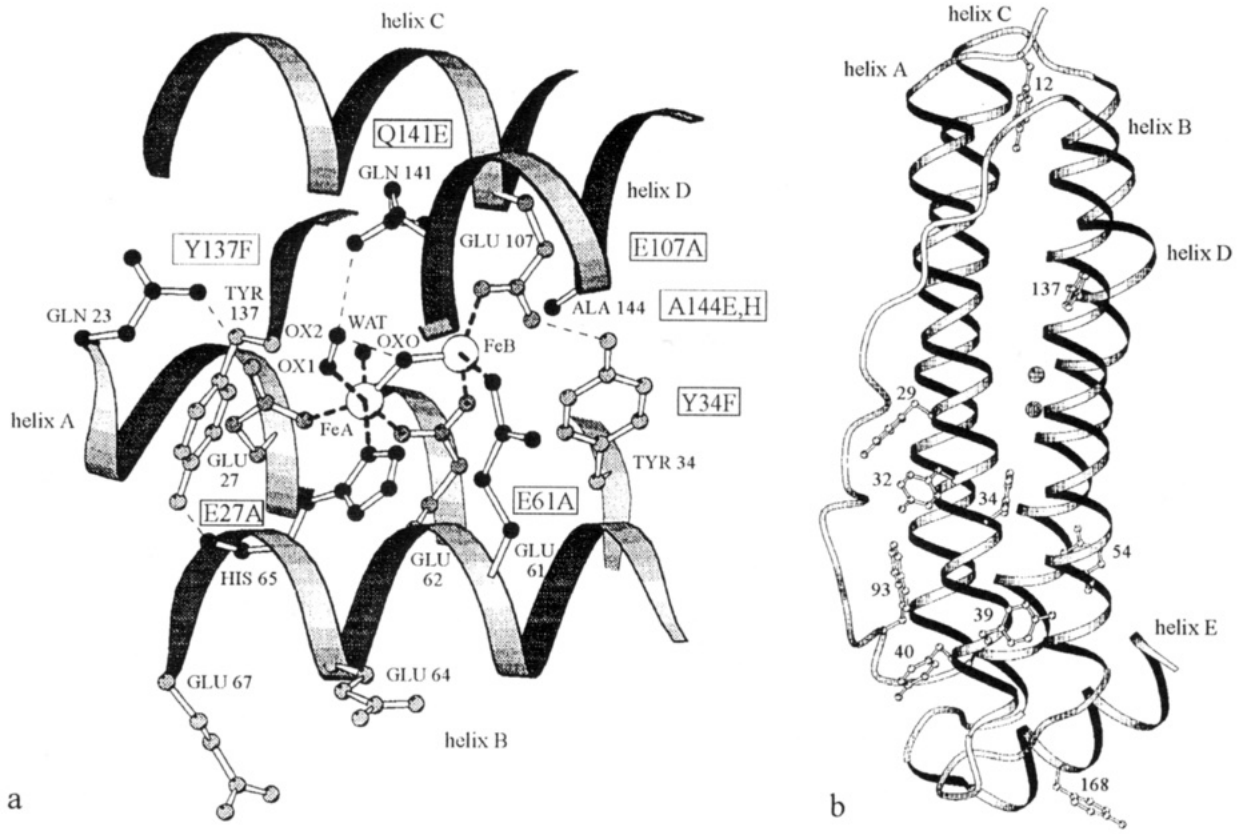

FIGURE 1: Diagrammatic drawings of (a) the ferroxidase center region and (b) the whole subunit of HuHF. (a) Iron dimer at the ferroxidase center of HuHF. The μ-oxo-bridged Fe(III) dimer modeled here [as in Treffry et al. (1992)] is an Fe(II) oxidation product obtained by binding O_2 asymmetrically to an Fe(II)/Fe(II) dimer similar to that of hemerythrin (Stenkamp et al., 1985). Alternatively, O_2 may bind symmetrically between two Fe(II) atoms to give a diferric μ-1,1-peroxide as in ribonucleotide reductase (Ling et al., 1994) or a diferric μ-1,2-peroxide as described for a model complex by Ménage et al. (1990). The Fe(III) positions are similar to those directly observed in EcFTN (Hempstead et al., 1994). The amino acid substitutions used in this study are shown boxed. Glu-61 shown as a ligand of FeB can take up an alternative position on the inside surface near Glu-64 (Lawson et al., 1991). (b) Ribbon diagram of an HuHF subunit showing all the tyrosine residues and the single tryptophan. Tyrosines 29, 32, 34, and 137 (which are common to BfHF) were changed individually to phenylalanine as was Trp-93. The spheres represent the Fe(III) atoms of the dimer, as modeled. The figures were prepared using the Molscript drawing program of Kraulis (1991).

the effects of site-specific mutagenesis. Amino acid sequence changes were made in several residues located in, or near to, the ferroxidase center, and in three aromatic residues lying near the outside of the shell (Figure 1). It was found that the rates of Fe(II) oxidation and/or the intermediates formed were affected only when residues participating directly in the ferroxidase center were altered.

The rates of HuHF-mediated oxidation of successive additions of 48 Fe(II) atoms/molecule were also investigated. It was found that the maintenance of fast rates of iron oxidation depended on the mobilization of the oxidized iron from the ferroxidase centers.

MATERIALS AND METHODS

Site-Directed Mutagenesis, Protein Purification, and Iron Removal. Site-directed mutagenesis, overproduction of HuHF and its variants in *Escherichia coli*, and purification of the ferritins were performed as described by Treffry et al. (1989). The HuHF and its derivatives, used in this study, contain a Lys-86 → Gln (K86Q) substitution that was included (originally) to induce crystallization (Lawson et al., 1991). Prior to their use, all ferritins were treated with sodium dithionite to remove endogenous iron (Treffry et al., 1992). Protein concentrations were determined using the Bio-Rad Dye Reagent with HuHF as a standard. The concentration of HuHF was determined by amino acid analysis. Horse spleen ferritin (HoSF) was obtained from Boehringer Mannheim (Lewes, East Sussex, U.K.), and its iron was removed with dithionite according to Bauminger et al. (1991). HoLF was a gift from Drs. K. Nagayama and S. Ebina of the Nagayama Protein Array Project, Tsukuba, Japan.

Rapid Kinetic Experiments. Rapid kinetic experiments were carried out using the SX.17MV stopped-flow instrument (Applied Photophysics, Leatherhead, U.K.), fitted with the SpectraKinetics facility (to enable time-resolved spectra to be collected) and a sequential mixing option. To facilitate the recording of data over relatively long periods (50 s), as well as obtaining good information for the fast phase of oxidation, 1000 data points were collected using the logarithmic collection mode. Unless otherwise stated, all quoted concentrations are the final concentrations after mixing. In a typical absorbance study, Fe(II), at 48 Fe atoms/molecule (96 μM), was mixed with an equal volume of a 1 mg/mL (2 μM) solution of protein in 0.2 M Mes buffer (pH 6.5). In fluorescence experiments, the protein concentration before mixing was reduced to 0.25 mg/mL, such that the linear range of the fluorescence response was not exceeded, and 48 Fe(II) atoms/molecule were added as before. The excitation wavelength was 280 nm, and emission was measured using a filter which cuts off all light below 320 nm. Fe(II) was added as ammonium ferrous sulfate (99.997%

pure, Aldrich Chemical Co., Dorset, England). Stock solutions of Fe(II) were prepared in 5 mM H_2SO_4 and diluted in 50 μM H_2SO_4 immediately prior to use. All stopped-flow experiments were carried out at a constant temperature of 23 °C.

Initial rates were obtained as the slopes to the initial, linear proportion of the change in optical absorbance (after the lag phase) following addition of Fe(II), recorded at 550 and 330 nm. At the lowest Fe(II) concentration (12 μM), the linear part of the curve was from 0.028 to 0.120 s, and at the highest concentration of Fe(II) used (192 μM), from 0.01 to 0.03 s.

Residual Fe(II) was measured using the sequential mixing facility. In this mode, the protein was reacted initially with the iron solution and then held in an aging loop for various times before being mixed with an equal volume of 1 mM 1,10-phenanthroline, in 0.1 M Mes buffer, and the absorbance of the Fe(II)−(phenanthroline)$_3$ complex measured at 510 nm. Fe(II) available to 1,10-phenanthroline was calculated as the amount of Fe(II) reacting with it 0.1 s after being mixed with the chelator. Total Fe(II) was calculated from the amount of Fe(II) reacting with 1,10-phenanthroline after the Fe(II) was first mixed with buffer alone.

Stopped-Flow Photodiode-Array Spectroscopy. A photodiode-array detector, recently available for the Applied Photophysics SX.17MV stopped-flow instrument, was used to generate spectra between 380 and 800 nm, resulting from the oxidation of 48 Fe(II) atoms/molecule by HuHF (6.5 μM protein, 312 μM Fe(II), pH 6.5). Four hundred data points were collected over 50 s using a pseudo-logarithmic collection mode. In this mode, the frequency of data points, at the beginning, is limited by the response time of the photodiode array (2.64 ms).

Manual Fe(II) Oxidation Experiments. Solutions of apo-HuHF or its variants [0.4 mL of a 10 mg/mL solution (20 μM)] were mixed with 5 μL of 76.8 mM $(NH_4)_2Fe(SO_4)_2$, in 1 mM H_2SO_4, and examined for the appearance of color.

Measurements of Oxygen Consumption. Oxygen consumption was measured with a Clark-type oxygen electrode having an electrode compartment of 1.5 mL. The protein, 1.5 μM in 0.1 M Mes buffer (pH 6.5) at 25 °C, was equilibrated with air before the compartment was closed and Fe(II), usually 48 Fe(II) atoms/molecule (as 5 μL in 1 mM H_2SO_4), was added. Oxygen consumption was recorded using an X-Y recorder, and the initial rates of consumption were calculated from a tangent to the initial part of the progress curve. Immediately after the complete oxidation of the first sample of Fe(II) (usually within the first minute), a second sample of Fe(II) was added and the initial rate of oxygen consumption measured again. For experiments in which restoration of activity was measured over longer periods, 48 Fe(II) atoms/molecule (or more, as specified) were added to the apoferritin (5.6 μM protein), and thereafter, samples were taken at intervals and equilibrated in the oxygen electrode compartment and the rates of oxygen consumption measured for the oxidation of a further 48 Fe(II) atoms/molecule. The results are expressed as a percentage of the rate observed with the first addition of 48 Fe(II) atoms/molecule to the apoferritin.

In some experiments, HoLF containing a small iron core (150 Fe atoms/molecule) was added to the HuHF before the first addition of iron. The reconstitution of iron cores in HoLF was carried out according to Bauminger et al. (1994).

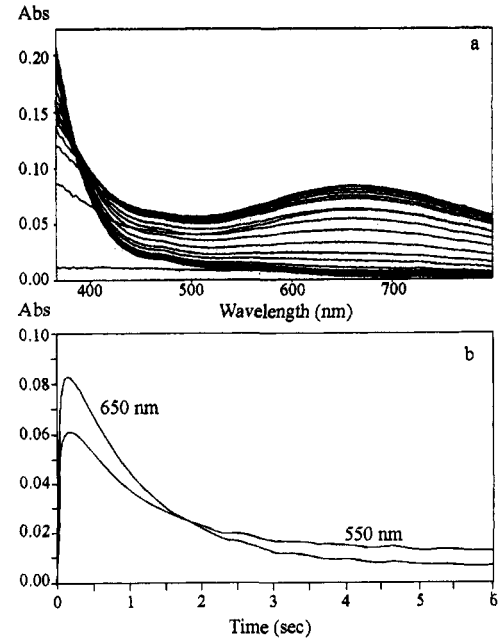

FIGURE 2: Oxidation of 48 Fe(II) atoms/molecule by apo-HuHF. (a) Spectra (380−780 nm) resulting from the oxidation of 48 Fe(II) atoms/molecule by HuHF (6.5 μM protein, 312 μM Fe(II), 0.1 M Mes buffer, pH 6.5) obtained using the photodiode-array spectrophotometer. Four hundred spectra were collected over 50 s using a pseudo-logarithmic collection mode; every 10th spectrum is shown here. (b) Comparison of the progress curves at 550 and 650 nm obtained with the photodiode-array spectrophotometer.

RESULTS

Absorption Spectra Produced by the Oxidation of 48 Fe(II) Atoms/Molecule by HuHF Recorded with a Photodiode-Array Stopped-Flow Spectrophotometer. The oxidation of 48 Fe(II) atoms/molecule by apo-HuHF produces a transient blue species with an absorbance maximum at 650 nm (Figure 2a). At a protein concentration of 3.25 μM, maximum absorbance (throughout the range of 360−780 nm) was reached at 0.14 s and declined thereafter, whereas absorbance in the near-UV increased continuously. It is apparent that the blue species was being replaced by another which absorbs very little at the longer wavelengths (note the isosbestic point at about 380 nm). The broad absorbance in the visible region could be due to more than one component absorbing in this range. However, the entire visible absorbance first increased and then decreased together, implying that, if there are multiple components, some of them form and decay in parallel.

In other studies reported here, the absorbance at 550 nm was used to analyze the characteristics of the initial blue species, as in earlier studies of HuHF and BfHF (Bauminger et al., 1993; Waldo & Theil, 1993). Although the maximum absorbance was lower at 550 nm than at 650 nm, the rate of increase in absorbance is broadly similar at these wavelengths (Figure 2b).

Stopped-Flow Spectrophotometric Investigation of the Oxidation of 48 Iron Atoms/Molecule by Wild-Type Recombinant apo-HuHF. Iron oxidation was monitored indirectly, from the Fe(II) remaining in solution, and directly, by the appearance of oxidation products absorbing at 330 and 550 nm.

Residual Fe(II) was measured by its colored complex with 1,10-phenanthroline. In the presence of a 20-fold excess of

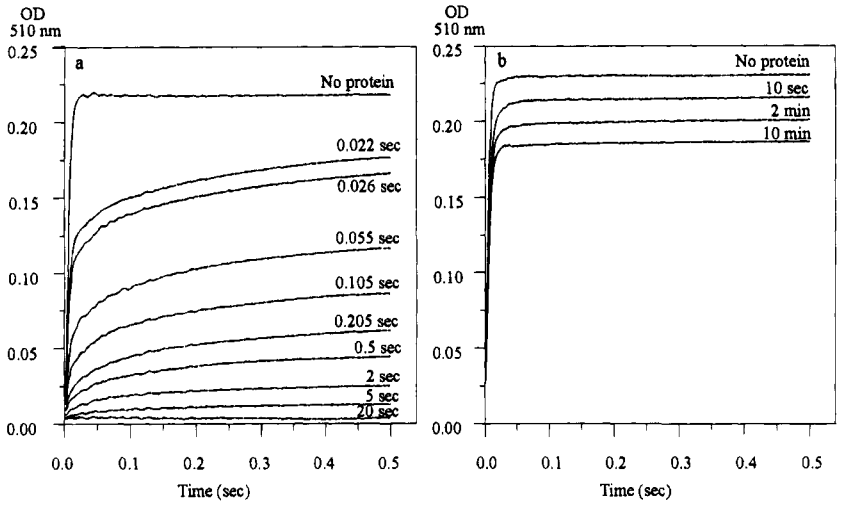

FIGURE 3: Availability of Fe(II) to 1,10-phenanthroline. Residual Fe(II) was measured at 510 nm as its colored complex with 1,10-phenanthroline using a sequential stopped-flow method. Apoferritins, (a) apo-HuHF and (b) apo-HoLF, were first mixed with an equal volume of Fe(II) and held in the aging loop for the times specified on each curve. The Fe−protein solutions were then mixed with an equal volume of 1,10-phenanthroline, and absorbance at 510 nm was recorded. Concentrations before the first mixing were as follows: 2 μM protein in 0.2 M Mes buffer (pH 6.5) and 96 μM Fe(II) as $(NH_4)_2Fe(SO_4)_2$ in 50 μM H_2SO_4. 1,10-Phenanthroline, 960 μM in 0.1 M Mes buffer (pH 6.5), was used in the second mixing. For the measurement of Fe(II) in the absence of protein, Fe(II) was first mixed with buffer, held in the aging loop for 22 ms, and then mixed with the phenanthroline solution.

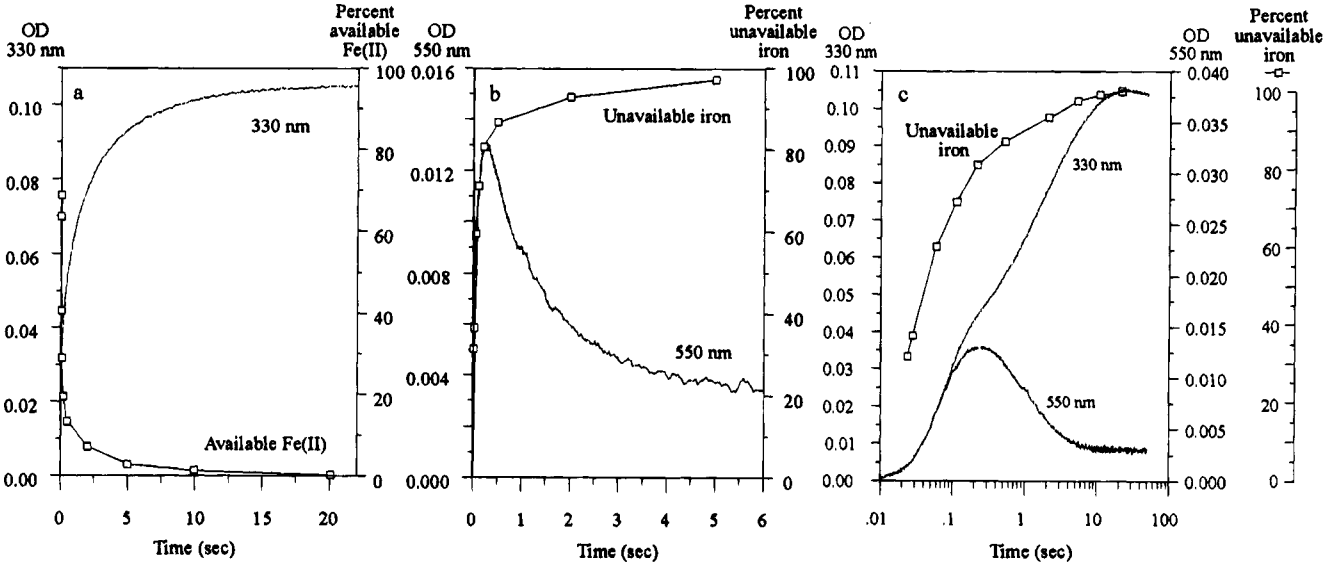

FIGURE 4: Stopped-flow kinetics of Fe(II) oxidation by HuHF. The amount of iron available for chelation by 1,10-phenanthroline (□), was measured using a sequential mixing mode as described in Figure 3. It was calculated from the amount of complex formed 0.1 s after mixing. The data are shown as remaining Fe(II) in part a and as a percentage of iron unavailable for complexation with 1,10-phenanthroline in parts b and c. Single wavelength kinetics were measured at (a) 330 and (b) 550 nm, using the single mixing mode, with 1 μM protein, 48 μM Fe(II), and 0.1 M Mes buffer (pH 6.5) (final concentrations). (c) Data from parts a and b replotted using a logarithmic time scale.

phenanthroline over iron, the Fe(II)−phenanthroline complex was fully formed within 25 ms (Figure 3). When Fe(II) was first mixed with apo-HuHF and then, after a delay of between 0.022 and 20 s, with 1,10-phenanthroline, Fe(II)−phenanthroline complex formation was clearly multiphasic with fast and slow components (Figure 3a). The fast component represents free Fe(II), some of it probably within the protein cavity. The slow component may represent Fe(II) initially bound to HuHF in the ferroxidase centers (prior to oxidation), which is stripped from the protein by the phenanthroline. This interpretation is supported by the absence of the slow component when Fe(II) is premixed with HoLF (Figure 3b), suggesting that in this case there is no protein-bound Fe(II) that is slowly made available to the chelator. Compared with the complete disappearance of Fe(II) within 20 s in the presence of HuHF (Figure 3a), the long-term availability of Fe(II) to phenanthroline in the presence of HoLF (over the 10 min of aging, Figure 3b) also suggests that any Fe(II) that has diffused into the protein shell, but is not bound by the protein, is available for fast reaction with 1,10-phenanthroline. The slight decrease in Fe(II) over 10 min (Figure 3b), as shown by the reduction in total absorbance at 510 nm, is likely to be due to its auto-oxidation and some oxidation within HoLF.

The time course of Fe(II) oxidation by HuHF, monitored at 330 nm, is compared with the loss of Fe(II) in Figure 4a. In each experiment, 48 Fe(II) atoms/molecule were added aerobically as $(NH_4)_2Fe(SO_4)_2$ to apo-HuHF (1 μM final concentration) in 0.1 M Mes buffer (pH 6.5). The data in Figure 4a suggest that, in the first 5 s, the disappearance of

Fe(II) is faster than the appearance of absorbance at 330 nm and that both processes are complete by 20 s. The fraction of iron unavailable to phenanthroline (calculated from the measured residual Fe(II) and much of it likely to be Fe(III)) is shown in Figure 4b and compared with the absorbance at 550 nm, measured over the first 6 s under the same conditions. The latter peaked at about 0.25 s, but declined to about 20% of its maximum value by 6 s. Figure 4b also shows that, when 48 Fe(II) atoms/molecule are added to HuHF, the absorbance at 550 nm reached a maximum when about 20% of Fe(II) is still available to 1,10-phenanthroline.

To emphasize the changes occurring within the first second following Fe(II) addition to apo-HuHF, the data were redrawn on a logarithmic time scale (Figure 4c). A number of features that were not obvious in Figure 4a,b become apparent. The plot of 330 nm absorbance shows an initial lag of 10−20 ms and an inflection at a time (ca. 0.25 s) when the increase in 330 nm absorbance is slightly less than half-maximal. This indicates (as already shown by the spectra of Figure 2a) that there is more than one species absorbing at 330 nm and also that there is a delay before the first species is formed. Note that the inflection in the 330 nm time course occurs at the time when the 550 nm absorbance is maximal (Figure 4c) and that the delay in appearance of the absorbance at 550 nm is of the same time scale as that at 330 nm. These findings, together with the observation that the absorbance at 330 nm continues to increase while that at 550 nm diminishes, suggest the following interpretation. A species absorbing at near-UV and visible wavelengths is formed first and then gradually declines between about 0.2 and 10 s, to be replaced by one or more species absorbing only in the near-UV region. Measurements of residual Fe(II) indicate that it becomes unavailable to 1,10-phenanthroline rather more rapidly than the formation of the "330/550 nm" complex. This again suggests that initially Fe(II) becomes unavailable through binding to the protein before it is oxidized. The absorbance at 550 nm reaches a maximum when approximately 80% of the iron is unavailable to the chelator. The loss of the last 20% of the Fe(II) coincides with the continuing rise in absorbance at 330 nm. This 330 nm absorbance may therefore have one component arising from oxidation of the remaining Fe(II) and another by transformation of the initial 330/550 nm complex.

Stoichiometry of the Species Absorbing at 330 and 550 nm. The dependence of initial rates of absorbance changes on the iron added per molecule was investigated at fixed protein (1 μM) and variable Fe(II) concentrations. Double reciprocal plots of the initial rates vs Fe concentration were nonlinear (Figure 5a). However, linear relationships were found at both wavelengths, when $1/v$ was plotted vs $1/[Fe]^2$ (Figure 5b). These data clearly indicate that an initial complex absorbing at both 330 and 550 nm is formed by concerted oxidation of two Fe(II) atoms. Pairwise oxidation is supported by data obtained from two successive additions of 24 Fe(II) atoms/molecule (the second after a 10 min interval) (Figure 6). The similar changes in absorbance at 330 and 550 nm observed for the two additions indicate that the oxidation of the second 24 Fe(II) atoms is essentially independent of the first.

Origin of the Visible Absorbance: Effect of Amino Acid Substitutions. It has been reported previously that no species absorbing at 550 nm is seen with HuHF variants Y34F,

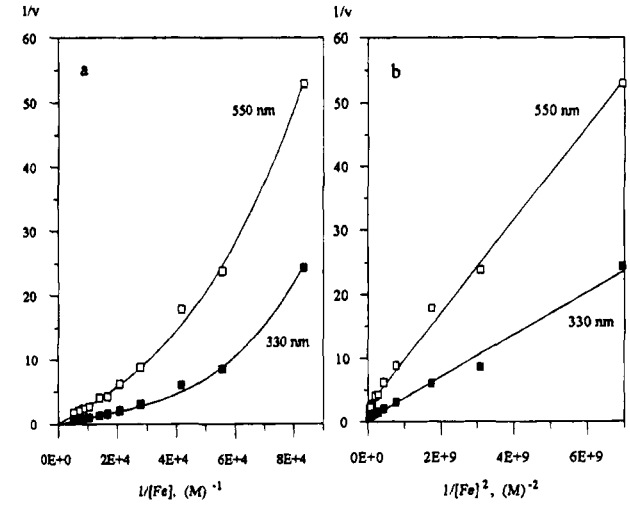

FIGURE 5: Dependence of initial rates of product formation on Fe(II) concentrations: (a) $1/v$ vs $1/[Fe(II)]$ and (b) $1/v$ vs $1/[Fe(II)]^2$. The initial rates, v, were calculted from the linear proportion of the initial reaction as described in Materials and Methods. The linear dependence of product formation on $1/[Fe(II)]^2$, at both 550 and 330 nm, suggests that they are the result of cooperative binding and oxidation of two Fe(II) atoms.

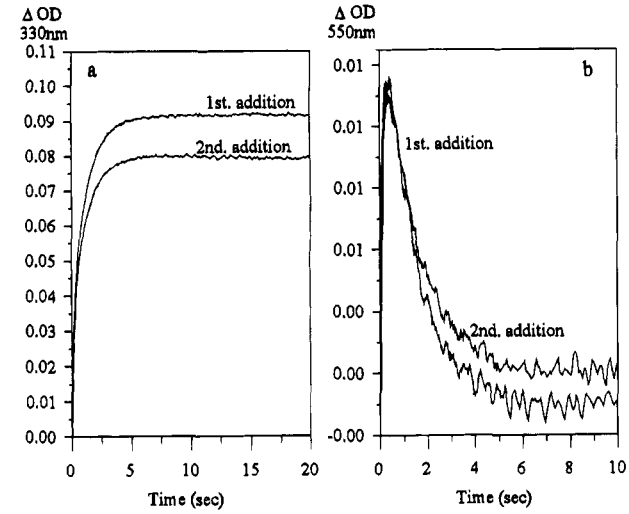

FIGURE 6: Oxidation of two consecutive additions of 24 Fe(II) atoms/molecule by HuHF measured at (a) 330 and (b) 550 nm. The reactions were done in the sequential mode. To measure the rate of oxidation of the first 24 Fe(II) atoms/molecule, 4 μM apo-HuHF in 0.2 M Mes buffer (pH 6.5) was mixed with an equal volume of the same buffer, and after 10 min, it was mixed again with an equal volume of 48 μM Fe(II) in 50 μM H_2SO_4 and the change in absorbance recorded. To measure the rate of oxidation of the second 24 Fe(II) atoms/molecule, 4 μM apo-HuHF in 0.2 M Mes buffer was mixed first with an equal volume of 96 μM Fe(II) solution, and after 10 min, the Fe−protein solution was mixed again with 48 μM Fe(II) (equal volume) and the change in absorbance recorded.

E27A, or Q141E (Bauminger et al., 1993; Harrison et al., 1994). This was confirmed here in both manual-mixing and stopped-flow experiments. In the former, the faint and transient blue color observed when 48 Fe(II) atoms/molecule were mixed with apo-HuHF was not seen with the Y34F or Q141E variants.

Time-resolved stopped-flow-generated spectra are shown for selected variants in Figure 7a−c. Of the tyrosine variants examined, only Y34F gave no significant visible absorbance (Figure 7b); Y29F (Figure 7a), Y32F, and Y137F (not shown) were similar to HuHF (not shown, but see Figure

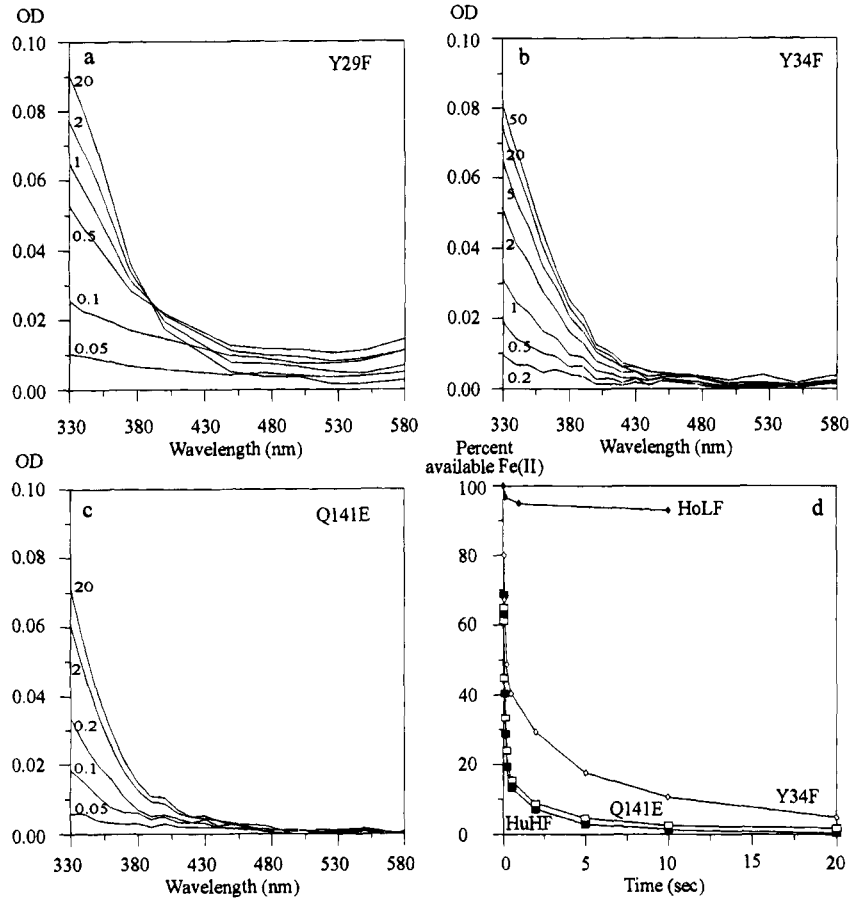

FIGURE 7: Disappearance and oxidation of 48 Fe(II) atoms/molecule in the presence of apo-HuHF and its site-directed variants. (a–c) Time-resolved spectra. The number by each spectrum represents the time, in seconds, at which the spectrum was calculated. (d) Residual Fe(II) measured as its availability to 1,10-phenanthroline. Residual Fe(II), in the presence of HoLF, is also shown. Time-resolved spectra were reconstructed from kinetic data measured at 10 nm intervals in the range of 330–580 nm using the software provided by Applied Photophysics. Conditions were as in Figure 4. Residual Fe(II) was measured as described in the legend to Figure 3. Fe(II) disappearance with Y29F was indistinguishable from that with HuHF (not shown).

2a for photodiode-array spectra). Tyr-29 and Tyr-32 are conserved tyrosines in the A helix near the outside of the protein shell, whereas Tyr-137 lies on the D helix near the ferroxidase center (Figure 1b). Changing the only tryptophan (W93F), located near Y29 and Y32 and also highly conserved in vertebrate ferritins, was again without effect (not shown). Ala-144 is close to Tyr-34 and to FeB of the proposed dinuclear iron center (Figure 1a). Variant A144E showed only 30% of the absorbance change, at 550 nm, as compared to the wild-type protein, but normal absorbance change was observed with A144H (data not shown). Glu-61 is an optional ligand of FeB (Figure 1a), but an E61A replacement had no effect on the 550 nm species (not shown).

Is the Formation of the "550 nm" Species an Essential Step in the Catalytic Oxidation of Fe(II)? Certain residue changes are associated with both slow Fe(II) oxidation and the failure to observe the 550 nm absorbance. However, fast Fe(II) binding and oxidation can occur without the appearance of absorbance at 550 nm. Rates of Fe(II) disappearance with Q141E and Y34F are compared with data for HuHF and HoLF in Figure 7d. When Fe(II) was mixed with HoLF, which has no di-iron centers and no ferroxidase activity, 93% of the iron was still available to 1,10-phenanthroline at 10 s. In contrast, with HuHF, the rapid decline of available Fe(II), to only about 10% at 2 s, is consistent with the conclusion that the initial binding of Fe(II) occurs at the ferroxidase centers. Fe(II) binding was not affected by the amino acid substitutions Q141E [or E61A (data not shown)], but there seems to be rather more Fe(II) available to 1,10-phenanthroline at 22 ms (dead time of the experiment) in the presence of Y34F than in the presence of HuHF, suggesting weaker binding of Fe(II) by this variant. The lag before the absorbance at 330 nm increased was also longer for Fe(II) oxidation by Y34F than by HuHF or Q141E (Figure 8a). The spectra in Figure 7b,c indicate that, while the visible component is virtually absent from Q141E and Y34F, the absorbance in the 330–450 nm region increases during the 20 s following addition of Fe(II), concomitant with Fe(II) oxidation. The total absorbance in the near-UV in Q141E seemed to be somewhat lower than that of HuHF (Figure 8a), implying that the oxidation of 48 Fe atoms/molecule yields a product having slightly different characteristics. However, the data in Figures 7d and 8a indicate that the rates of Fe(II) binding and oxidation are similar for HuHF and Q141E. Thus, although the formation of a species responsible for the visible absorption occurs as one of the first steps in HuHF, and is dependent on ferroxidase center residues (except Glu-61), it is apparently not essential for the catalysis.

Measurement of Fluorescence Quenching by Iron. The effects of iron on protein fluorescence were compared to changes in absorbance at 330 nm due to iron oxidation. Time courses were recorded for 330 nm absorbance with HuHF and several variants (Figure 8a) and for fluorescence quench-

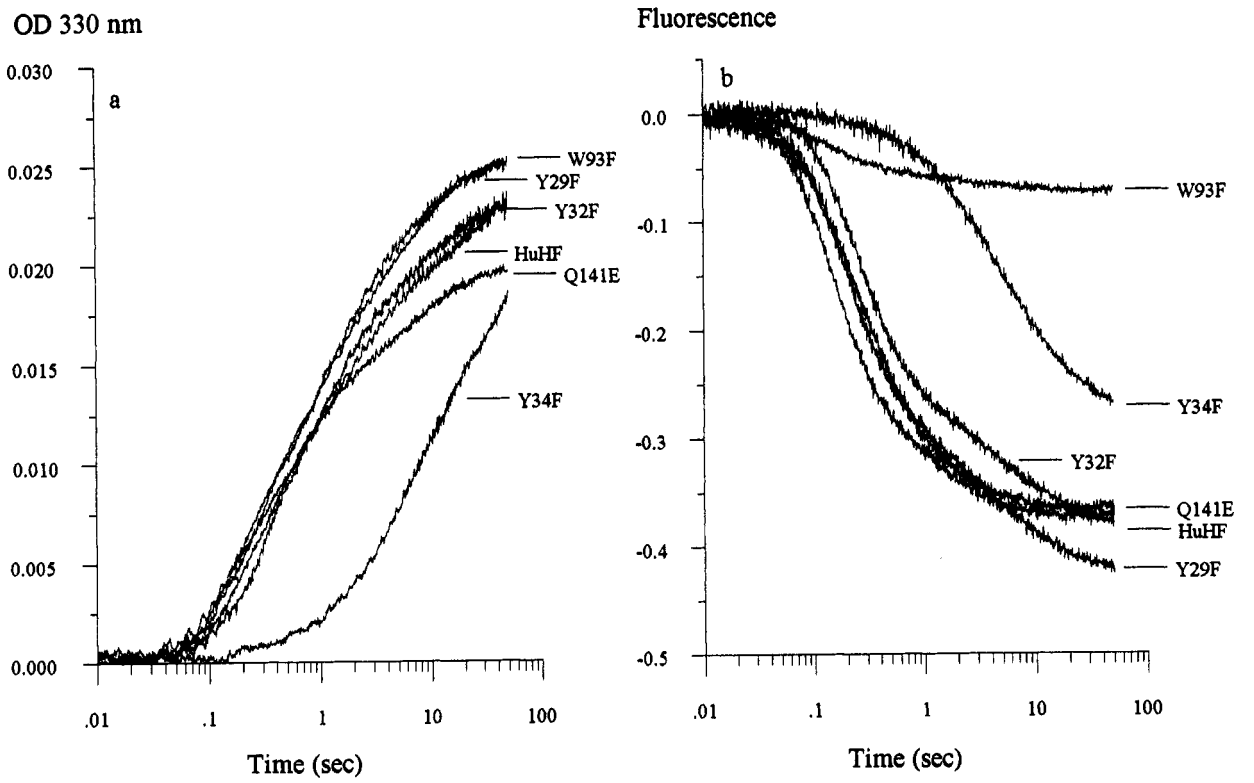

FIGURE 8: Comparison of changes in absorbance at 330 nm (a) and fluorescence (b) after addition of 48 Fe(II) atoms/molecule. Absorbance and fluorescence measurements were done at the same protein concentrations [0.25 μM protein in 0.1 M Mes buffer (pH 6.5) and 12 μM Fe(II) (final concentrations)]. For the fluorescence measurements, the protein solutions were excited at 280 nm and the decrease in fluorescence was measured (after setting protein fluorescence to zero) using a filter which cut off all light below 320 nm.

ing by iron (Figure 8b, the intrinsic fluorescence of the proteins was set to zero). The same lag phase observed with absorbance (Figures 4c and 8a) was observed for fluorescence quenching (Figure 8b). Thus, in HuHF, the quenching of fluorescence appears not to be reporting on a binding step that precedes oxidation. However, comparison of fluorescence quenching with the absorbance at 330 nm, when 48 Fe(II) atoms/molecule are added to HuHF (Figure 8), shows that the change in fluorescence is complete in about 10 s, whereas the absorbance at 330 nm is still increasing at 50 s. This suggests that most of the quenching is due to an early intermediate in the oxidation reaction. Variant E27A exhibited no fluorescence quenching when Fe(II) was added and little or no oxidation (data not shown). Variants Y137F (not shown), Y29F, Y32F, and Q141E behaved like HuHF in both fluorescence and 330 nm absorbance properties. However, Y34F and W93F did not fit this pattern. In Y34F, both absorbance change (330 nm) and fluorescence quenching were slow. In W93F, the absorbance change was similar to that of HuHF, but overall protein fluorescence (not shown) and the degree of quenching by iron (Figure 8b) were low, indicating that in HuHF this single tryptophan gives most of the protein fluorescence and is subject to most of the quenching. The two iron atoms of the proposed dinuclear site are located 10−12 Å from Trp-93, a distance over which energy transfer is possible. The remaining fluorescence due to tyrosines is also quenched by the products of iron oxidation. It is interesting to note, though, that, even when the contribution from tryptophan fluorescence is removed, as in W93F, the progress curves of absorbance and fluorescence still show the same lag phase. This indicates that, like the quenching of tryptophan, the quenching of the tyrosine fluorescence is not due to Fe(II) binding prior to oxidation.

Successive Additions of 48 Fe(II) Atoms/Molecule. In contrast to the two consecutive additions of 24 Fe atoms/molecule, where the absorbance changes for the two additions were similar (Figure 6), differences were observed in the oxidative behavior of HuHF, when two additions of 48 Fe(II) atoms/molecule were made 10 min apart (Figure 9). The 330 nm absorbance developed more rapidly after the first addition of 48 Fe(II) than after the second, and the total absorbance reached at 20 s was less for the second addition (Figure 9a). Oxidation of the second 48 Fe(II) atoms/molecule gave no transient absorbance at 550 nm (Figure 9b). However, iron oxidation was still relatively fast, with 97% of the iron unavailable to 1,10-phenanthroline by 20 s (Figure 9c).

Regeneration of Fe(II) Oxidation Activity Measured as Oxygen Consumption. The initial rate of oxygen consumption was used as an estimate of ferroxidase activity. Activities for a second addition of 48 Fe(II) atoms/molecule, made at various intervals after the first and expressed as a percentage of the rate of the first addition, are shown in Table 1. With HuHF, a second addition made at 24 h gave only 71% of the initial rate of the first, but with Y34F, 100% restoration of activity was achieved by 6 h, although the actual rates of O_2 consumption were somewhat less than those of HuHF.

Recovery of activity in HuHF was faster when it was preloaded with 96 Fe atoms/molecule or when HoLF containing 150 Fe atoms/molecule was added (HoLF on its own gave no measurable rate of oxygen consumption). HoSF, which contains 21 L chains and only about 3 H chains,

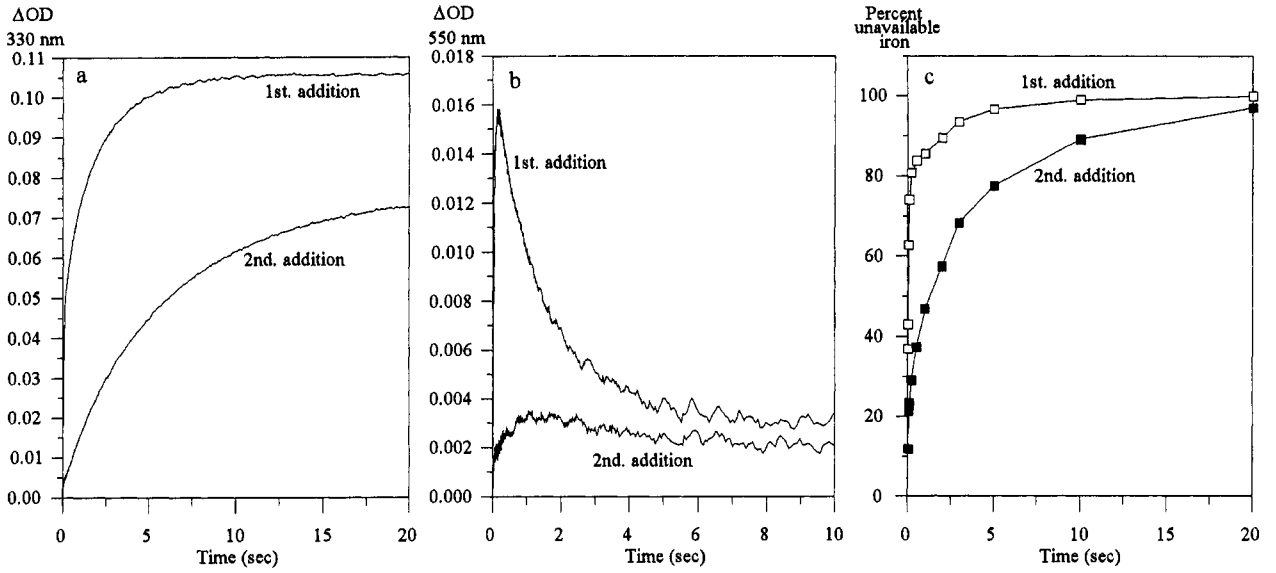

FIGURE 9: Oxidation, by HuHF, of two consecutive additions of 48 Fe(II) atoms/molecule. (a) Progress curves at 330 nm, (b) progress curves at 550 nm, and (c) percentage of Fe(II) unavailable to 1,10-phenanthroline. Conditions were as described in Figure 5 except that the first Fe(II) solution was 192 μM and the second 96 μM. The two additions were done at 10 min intervals. To measure the amount of Fe(II) available to 1,10-phenanthroline after the second addition of Fe, the apo-HuHF was preloaded with 48 Fe(II) atoms/molecule and the sample was then transferred into the syringes of the stopped-flow machine.

Table 1: Recovery of Ferroxidase Activity[a]

	percentage of original activity				
time[b] (h)	HuHF	96 Fe/HuHF	HuHF + 150 Fe/HoLF	Y34F	HoSF
0.05	32	ND[c]	30	21	42
1	28	40	56	40	96
6	38	100	88	100	93
24	71	105	100	110	ND[c]

[a] Ferroxidase activity was measured as the initial rate of O_2 consumption (with a Clark-type oxygen electrode) after addition of 48 Fe(II) atoms/molecule (except in HoSF where only 24 Fe atoms/molecule were added). The initial rates of a second addition were compared, in each case, with that measured after the first addition of 48 Fe atoms/molecule to the apoferritins. Detailed experimental conditions are described in Materials and Methods. Proteins, 1.5 μM in 0.1 M Mes buffer (pH 6.5) (3 μM HoSF), were placed in the reaction chamber, 1.5 mL total volume, and Fe(II) was added to give a final concentration. of 72 μM. The initial rates of oxygen consumption for the first addition of 48 Fe(II) atoms/molecule were found to be 10 ● 2, 3.2, and 1 ± 0.2 μM/s for HuHF, Y34F, and HoSF, respectively. Assuming 2 Fe(II) oxidized/O_2 molecule, this gives 13.3 μM Fe(II) s^{-1} (μM HuHF)$^{-1}$ (for 48 Fe(II) atoms/molecule). This value is much lower than the initial value for Fe(II) disappearance obtained from Figure 4 [e.g. from 0 to 0.055 s, 416 μM Fe(II) s^{-1} (μM HuHF)$^{-1}$] but is similar to the value of Fe(II) disappeared in the first 2 s [18 μM Fe(II) s^{-1} (μM HuHF)$^{-1}$]. It is apparent therefore that the oxygen electrode greatly underestimates initial rates, but as all measurements are carried out under the same conditions, the relationship between the recoveries obtained at successive times is probably correct. [b] Time after the first addition of Fe(II). [c] ND means not done.

also gave faster recovery rates, over 90% of the initial rate 1 h after the first addition (Table 1). From these results, it is apparent that regeneration of ferroxidase activity is assisted by the presence of a preformed iron core and possibly also of L chains in the same or in separate molecules.

DISCUSSION

Fe(II) oxidation by apo-HuHF, monitored by absorbance increases at 330 or 550 nm (Figures 4–8a) or by quenching of protein fluorescence (Figure 8b), begins after an initial time lag of about 10–20 ms. Since the data of Figure 4c show that in the presence of HuHF 30% of Fe(II) becomes unavailable to 1,10-phenanthroline within this period (probably due to binding to the protein), the lag may indicate that a conformational or other change occurs prior to its oxidation and/or that the first product does not absorb light in the wavelength range used here.

The replacement of the initial visible absorption by a second species with different absorbance characteristics indicates further chemical reaction and/or rearrangement of the Fe(III) atoms. This must occur faster than any further formation of the visible component. Results with HuHF variants indicate that formation of a colored component may be bypassed without reduction of overall reaction rate (e.g. Q141E, Figure 7c,d). It may be noted that EcFTN which also gives no initial colored complex oxidizes Fe(II) as fast as HuHF (A. Treffry, Z. Zhao, M. A. Quail, A. J. Hudson, J. R. Guest, and P. M. Harrison, unpublished observations). The major species present in HuHF at 20 s is likely to be the μ-oxo-bridged dimer identified by Mössbauer spectroscopy at 30–60 s (Bauminger et al., 1991, 1993, 1994).

The chemical nature(s) of the transient blue species has not yet been ascertained. Its bluish color and absorption maximum at 650 nm distinguish it from the purple species observed in BfHF and assigned as a tyrosinate → Fe(III) charge transfer complex on the basis of its resonance Raman modes (Waldo et al., 1993). A weak, flat absorbance extending into the visible spectrum (maximum at 570 nm) has been observed in stearoyl-ACP desaturase, another protein known to contain dinuclear iron, but not reported to have an Fe(III) bound to tyrosine (Fox et al., 1994). This absorbance and another weak band at 470 nm [also seen in heme-free variant of EcBFR (Andrews et al., 1995)] are thought to have contributions from charge transfer and ligand field transitions associated with the di-iron center. A very weak band at 470 nm is also seen with HuHF after the oxidation of 48 Fe(II) atoms/molecule and is most obvious at 50 s when a very faint shoulder at about 550 nm is also discernible (Figure 2a). A wide variety of other species are

known to absorb in the 400−800 nm region of the spectrum, including the purple and pink forms of uteroferrin (Antanaitis et al., 1983), tryptophan cation and tyrosine radicals (Butler et al., 1982), diferric−peroxo complexes (Ménage et al., 1990; Dong et al., 1993; Liu et al., 1995), a mononuclear alkylperoxoiron(III) complex [maximum at 640 nm (Ménage et al., 1995)], and Fe(III) derivatives of catecholic siderophores (Atta et al., 1993). A significant contribution of tryptophan radicals can be ruled out since variant W93F gives a normal initial spectrum (not shown). However, there is EPR evidence of production of a transient radical with axial symmetry ($g_{\parallel} = 2.042$, $g_{\perp} = 2.0033$) during the first second of Fe(II) oxidation by horse spleen apoferritin (Sun & Chasteen, 1994). This radical is as yet unidentified, but it is considered to be due to tyrosine, histidine, cysteine, or methionine, but not tryptophan.

The present study confirms and extends the previous conclusion (Bauminger et al., 1993; Harrison et al., 1994) that the presence of ferroxidase center residues is required for the production of the initial visible species (except for Glu-61 which seems not to be essential for binding Fe at site B). In the crystal structure of HuHF, Glu-61 occupies alternative positions, only one of which binds FeB of the proposed dinuclear center (Lawson et al., 1991). In EcBFR, which gives no blue or purple complex (Le Brun et al., 1993), five of the seven ferroxidase center residues of HuHF are conserved, but residue 141 (H chain numbering) is Glu, not Gln, and 61 is Asp, not Glu (Andrews et al., 1992). His-144 is proposed to bind iron at site B instead of Glu-61 (Cheesman et al., 1992), and this residue is seen in the crystal structure to be a ligand of one of the two (unidentified) metal center ions (probably Mn^{2+}) in EcBFR (Frolow et al., 1994). In HuHF, the substitutions E61A and A144H are without effect on production of the 550 nm species, whereas Q141E, which introduces an additional negative charge, prevents its appearance and may explain its absence from EcBFR. In EcFTN, which again gives no blue absorbance, all seven ferroxidase center residues (including Tyr-34) are conserved (Hempstead et al., 1994). However, EcFTN has Glu-144 instead of Ala-144, again introducing an additional negative charge and a change which in HuHF abolishes the production of the visible species (not shown). Conversely, a blue absorbance has recently been generated in a variant of EcFTN having the changes E143K+E144A (A. Treffry, Z. Zhao, M. A. Quail, J. R. Guest, and P. M. Harrison, unpublished observation).

Substitutions Y29F, Y32F, and Y137F have no effect on the visible species, but it does not appear in variant Y34F (Figure 7); this is consistent with the direct involvement of Tyr-34 as an Fe(III) ligand and/or possibly in tyrosine radical production. However, the fast oxidation of iron by Q141E, and EcFTN, which do not show the blue species, suggests that the major role of Tyr-34 may be not in the direct binding of iron, but in the construction of a ferroxidase center with geometry poised to allow for fast oxidation of bound Fe(II) and/or in the shepherding of Fe(II) into its oxidation center. In the crystal structure of HuHF, Tyr-34 is seen to hydrogen bond to Glu-107, a residue crucial for fast oxidation (Bauminger et al., 1991, 1993). The hydrogen bond may allow for electron transfer in addition to its structural role. The blue species could be a diferric μ-peroxo complex, and the failure to observe it in variants Y34F, Q141E, and A144E (or in EcBFR and EcFTN) may be because it has decayed within the dead time of the spectrometer (3−4 ms). Alternatively, if it were an Fe(III)−tyrosinate, then the data of Figures 5 and 6 would suggest that it is a component of an Fe(III) dimer complex, as has been considered previously (Bauminger et al., 1993; Harrison et al., 1994). Nevertheless, the fluorescence-quenching data do not indicate quenching due to Fe(II) binding to tyrosine (Figure 8).

Further work (e.g. rapid freeze Raman and Mössbauer spectroscopy) may allow for the nature of the initial species to be determined. However, it is apparent that binding and oxidation of the first 48 Fe(II) atoms/molecule is a fast and highly cooperative process. This confirms earlier Mössbauer studies which showed that μ-oxo-bridged Fe(III) dimers form a substantial proportion of the product at 30−60 s even when only 10 or 12 Fe(II) atoms/molecule had been added (Bauminger et al., 1991, 1993, 1994). The essentially pairwise oxidation seen here is consistent with the proposal that two Fe(II) atoms are oxidized by a single O_2 molecule binding at the ferroxidase center (Treffry et al., 1992) and with measurements of oxidation stoichiometry, giving a value of approximately 2 Fe(II)/O_2 for oxidation on the protein shell (Treffry et al., 1978; Xu & Chasteen, 1991; Sun et al., 1993). Similar stoichiometries were observed for HuHF and its variants Q141E and Y34F (data not shown). Measurements (on HoSF) made in the presence of catalase or superoxide dismutase also indicated that H_2O_2, not O_2^-, is the product (Xu & Chasteen, 1991). Thus, Fe(II) oxidation in ferritin appears to differ from that at the dinuclear site of ribonucleotide reductase. In the latter, formation of the μ-oxo-bridged dinuclear Fe(III) complex, also highly cooperative, is accompanied by oxidation of a third Fe(II) at an unknown location, the reduction of dioxygen to water, and the production of a stable tyrosine radical (Ochiai et al., 1990; Bollinger et al., 1991; Nordlund et al., 1990). In HuHF, the iron core, once formed, provides an alternative site for Fe(II) oxidation, on which 4 Fe(II) can be oxidized per O_2 molecule with production of H_2O, not H_2O_2 (Macara et al., 1972; Treffry et al., 1978; Xu & Chasteen, 1991; Sun et al., 1993).

Experiments described here (Figure 9 and Table 1) and previously (Waldo & Theil, 1993) indicate that full restoration of ferroxidase activity, following an addition of 48 Fe(II) atoms/molecule, is slow. Tighter chelation of Fe(III) than of Fe(II) probably contributes to the ferroxidase effect, and the slow regeneration of activity may be due to the need to displace the dinuclear Fe(III) complex from the dinuclear center. Oxidation of a second increment of Fe(II), added 10 min after the first, may occur by a different mechanism since the product formed has different characteristics (no blue component and lower absorbance at 330 nm, Figure 9).

The presence of molecules containing iron cores significantly accelerates the restoration of ferroxidase activity, although this is still very slow in HuHF (Table 1). In HoSF (a mixed copolymer of about 15% H and 85% L subunits), extensive regeneration of activity occurs within only 1 h. This may be due to the more pronounced growth of iron cores within HoSF and hence of secondary iron-binding sites (Bauminger et al., 1991). The faster regeneration of ferroxidase activity observed here may also explain the efficiency of mixed human H/L copolymers in iron incorporation (Levi et al., 1993) and provide further rationale for the evolution of such copolymers in vertebrates. *In vivo*,

regeneration of activity may also be aided by the presence of small chelators, which can remove Fe(III) from the ferroxidase centers and carry it into the cavity. Moreover, if stable ferrihydrite nuclei, once formed within ferritin, can provide sites for binding Fe(III) and for Fe(II) oxidation, then rapid turnover of the ferroxidase centers may become unnecessary.

ACKNOWLEDGMENT

We are grateful to Dr. P. Arosio for the gift of W93F, Drs. K. Nagayama and S. Ebina for a gift of HoLF, and Dr. P. Hempstead for the drawing of Figure 1b.

REFERENCES

Andrews, S. C., Arosio, P., Bottke, W., Briat, J.-F., Von Darl, M., Harrison, P. M., Laulhere, J.-P., Levi, S., Lobreaux, S., & Yewdall, S. J. (1992) *J. Inorg. Biochem. 48*, 161−184.

Andrews, S. C., Le Brun, N. E., Barynin, V., Thompson, A. J., Moore, G. R., Guest, J. R., & Harrison, P. M. (1995) *J. Biol. Chem 40*, 23268−23274.

Antanaitis, B. C., Aisen, P., & Lilienthal, H. R. (1983) *J. Biol. Chem. 258*, 3166−3182.

Atta, M., Lamarche, N., Battioni, J. P., Massie, B., Langelier, Y., Mansuy, D., & Fontecave, M. (1993) *Biochem. J. 290*, 807−810.

Bauminger, E. R., Harrison, P. M., Nowik, I., & Treffry, A. (1989) *Biochemistry 28*, 5486−5493.

Bauminger, E. R., Harrison, P. M., Hechel, D., Nowik, I., & Treffry, A. (1991) *Biochim. Biophys. Acta 1118*, 48−58.

Bauminger, E. R., Harrison, P. M., Hechel, D., Hodson, N. W., Nowik, I., Treffry, A., & Yewdall, S. J. (1993) *Biochem. J. 296*, 809−819.

Bauminger, E. R., Treffry, A., Hudson, A. J., Hechel, D., Hodson, N. W., Andrews, S. C., Levi, S., Nowik, I., Arosio, P., Guest, J. R., & Harrison, P. M. (1994) *Biochem. J. 302*, 813−820.

Bollinger, J. M., Jr., Edmondson, D. E., Huynh, B. H., Filley, J., Norton, J. R., & Stubbe, J. (1991) *Science 253*, 292−298.

Butler, J., Land, E. J., Prutz, W. A., & Swallow, J. (1982) *Biochim. Biophys. Acta 805*, 150−162.

Cheesman, M. R., Kadir, F. H., al-Basseet, J., al-Massad, F., Farrar, J., Greenwood, C., Thomson, A. J., & Moore, G. R. (1992) *Biochem. J. 286*, 361−368.

Dong, Y., Ménage, S., Brennan, B. A., Elgren, T. E., Ho, G. J., Pearce, L. L., & Que, L., Jr. (1993) *J. Am. Chem. Soc. 115*, 1851−1859.

Fox, B. G., Shaklin, J., Ai, J., Loehr, T. M., & Sanders-Loehr, J. (1994) *Biochemistry 33*, 12886−12886.

Frolow, F., Kalb, A. J., & Yariv, J. (1994) *Struct. Biol. 1*, 453−460.

Hanna, P. M., Chen, Y., & Chasteen, N. D. (1991) *J. Biol. Chem. 266*, 886−893.

Harrison, P. M., Bauminger, E. R., Hechel, D., Hodson, N. W., Nowik, I., Treffry, A., & Yewdall, S. J. (1994) *Adv. Exp. Med. Biol. 356*, 1−12.

Hempstead, P. D., Hudson, A. J., Artymiuk, P. J., Andrews, S. C., Banfield, M. J., Guest, J. R., & Harrison, P. M. (1994) *FEBS Lett. 350*, 258−262.

Jacobs, D., Watt, G. D., Frankel, R. B., & Papaefthymiou, G. C. (1989) *Biochemistry 28*, 9216−9221.

Kraulis, P. J. (1991) *J. Appl. Crystallogr. 24*, 946−950.

Lawson, D. M., Artymiuk, P. J., Yewdall, S. J., Smith, J. M., Livingstone, J. C., Treffry, A., Luzzago, A., Levi, S., Arosio, P., Cesareni, G., Thomas, C. D., Shaw, W. V., & Harrison, P. M. (1991) *Nature 349*, 541−544.

Le Brun, N. E., Wilson, M. T., Andrews, S. C., Guest, J. R., Harrison, P. M., Thomson, A. J., & Moore, G. R. (1993) *FEBS Lett. 333*, 198−202.

Levi, S., Luzzago, A., Cesareni, G., Cozzi, A., Franceschinelli, F., Albertini, A., & Arosio, P. (1988) *J. Biol. Chem. 263*, 18086−18092.

Levi, S., Santambrogio, P., Albertini, A., & Arosio, P. (1993) *FEBS Lett. 336*, 309−312.

Ling, J., Sahlin, M., Sjoeberg, B.-M., Loehr, T. M., & Sanders-Loehr, J. (1994) *J. Biol. Chem. 269*, 5595−5601.

Liu, K. E., Valentine, A. M., Qiu, D., Edmondson, D. E., Appelman, E. H., Spiro, T. G., & Lippard, S. J. (1995) *J. Am. Chem. Soc. 117*, 4997−4998.

Macara, I. G., Hoy, T. G., & Harrison, P. M. (1972) *Biochem J. 126*, 151−162.

Ménage, S., Brennen, B. A., Juarez-Garcia, C., Munck, E., & Que, L., Jr. (1990) *J. Am. Chem. Soc. 112*, 6423−6425.

Ménage, S., Wilkinson, E. C., Que, L., Jr., & Fontecave, M. (1995) *Angew. Chem., Int. Ed. Engl. 34*, 203−205.

Niederer, W. (1970) *Experientia 26*, 218−220.

Nordlund, P., Sjöberg, B. M., & Eklund, H. (1990) *Nature 345*, 593−598.

Ochiai, E. I., Mann, G. J., Graslund, A., & Thelander, L. (1990) *J. Biol. Chem. 265*, 15858−15861.

Rosenberg, L. P., & Chasteen, N. D. (1982) in *The Biochemistry and Physiology of Iron* (Saltman, P., & Hegenauer, J., Eds.) pp 405−408, Elsevier Biomedical, New York.

Stenkamp, R. E., Sieker, L. C., Jensen, L. H., Mccallum, J. D., & Sanders-Loehr, J. (1985) *Proc. Natl. Acad. Sci. U.S.A. 82*, 813−816.

Sun, S., & Chasteen, N. D. (1994) *Biochemistry 33*, 15095−15102.

Sun, S., Arosio, P., Levi, S., & Chasteen, N. D. (1993) *Biochemistry 32*, 9362−9369.

Treffry, A., Sowerby, J. M., & Harrison, P. M. (1978) *FEBS Lett. 95*, 221−224.

Treffry, A., Harrison, P. M., Luzzago, A., & Cesareni, G. (1989) *FEBS Lett. 248*, 268−382.

Treffry, A., Hirzmann, J., Yewdall, S. J., & Harrison, P. M. (1992) *FEBS Lett. 302*, 108−112.

Waldo, G. S., & Theil, E. C. (1993) *Biochemistry 32*, 13262−13269.

Waldo, G. S., Ling, J., Sanders-Loehr, J., & Theil, E. C. (1993) *Science 259*, 896−898.

Xu, B., & Chasteen, N. D. (1991) *J. Biol. Chem. 266*, 19965−19980.

Yang, C. Y., Meagher, A., Huynh, B. J., Sayers, D. E., & Theil, E. C. (1987) *Biochemistry 26*, 498−503.

BI9512556